Real-Time Multislice MRI During Continuous Positive Airway Pressure Reveals Upper Airway Response to Pressure Change

Weiyi Chen, MS,[1]* Emily Gillett, MD, PhD,[2,3] Michael C.K. Khoo, PhD,[4]

Sally L. Davidson Ward, MD,[2,3] and Krishna S. Nayak, PhD[1]

Purpose: To determine if a real-time magnetic resonance imaging (RT-MRI) method during continuous positive airway pressure (CPAP) can be used to measure neuromuscular reflex and/or passive collapsibility of the upper airway in individual obstructive sleep apnea (OSA) subjects.

Materials and Methods: We conducted experiments on four adolescents with OSA and three healthy controls, during natural sleep and during wakefulness. Data were acquired on a clinical 3T scanner using simultaneous multislice (SMS) RT-MRI during CPAP. CPAP pressure level was alternated between therapeutic and subtherapeutic levels. Segmented airway area changes in response to rapid CPAP pressure drop and restoration were used to estimate 1) upper airway loop gain (UALG), and 2) anatomical risk factors, including fluctuation of airway area (FAA).

Results: FAA significantly differed between OSA patients (2–4× larger) and healthy controls (Student's t-test, $P < 0.05$). UALG and FAA measurements indicate that neuromuscular reflex and passive collapsibility varied among the OSA patients, suggesting the presence of different OSA phenotypes. Measurements had high intrasubject reproducibility (intraclass correlation coefficient $r > 0.7$).

Conclusion: SMS RT-MRI during CPAP can reproducibly identify physiological traits and anatomical risk factors that are valuable in the assessment of OSA. This technique can potentially locate the most collapsible airway sites. Both UALG and FAA possess large variation among OSA patients.

Level of Evidence: 1
Technical Efficacy: Stage 1

Obstructive sleep apnea (OSA) is a very common sleep disorder in the United States,[1] with a prevalence of 4–9% in adults and 2% in children.[2] OSA places a substantial financial burden on society, with the cost of untreated OSA estimated to be US$67–165 billion.[3] Untreated OSA can contribute to the development of hypertension,[4] coronary artery disease,[5] congestive heart failure,[6] arrhythmias,[7] stroke,[8] glucose intolerance, and diabetes.[9,10] OSA is characterized by repetitive cessation of airflow due to physical narrowing or collapse of the airway as a result of anatomical and physiological abnormalities in pharyngeal structure.[11] This collapse is typically attributed to excessive soft-tissue elements, such as the tongue, velum, uvula, and epiglottis, and/or increased collapsibility of the pharyngeal airway.[12]

Three-dimensional static magnetic resonance imaging (MRI) provides superb contrast and resolution to reveal the anatomical structures that potentially contribute to airway collapse.[13,14] Respiratory-gated CINE techniques have also been proposed to measure the airway change during tidal breathing, where multiple respiratory cycles are used to form one cycle of dynamic images.[15] Recently, 3D real-time MRI (RT-MRI) during natural sleep[16] and 2D RT-MRI during wakefulness[17] have been demonstrated alongside synchronized recording of physiological signals similar to

polysomnagraphy (PSG). These techniques have demonstrated a unique ability to identify airway collapse sites during natural sleep.

PSG is the standard technique for the diagnosis of sleep apnea, involving monitoring and recording multiple physiological signals in parallel that together reflect sleep physiology.[18] Research PSG can utilize a sealed facemask connected to a positive/negative pressure source to enable rapid switching between pressure levels so as to emulate the collapse of the upper airway (UA) during sleep. However, as PSG lacks visualization of pharyngeal structures, they cannot provide any information regarding the position and level of airway narrowing or collapse. Prior studies[16,17] have applied inspiratory occlusion, such as the Mueller maneuver (MM), to observe airway collapsibility during simultaneous dynamic MRI and PSG. However, MM is a voluntary effort with poor reproducibility.[19] Previous studies[20] have also shown that MM is inherently unable to identify all types of collapse.[21]

Continuous positive airway pressure (CPAP) acts as a pneumatic splint to prevent upper airway collapse and has been proven to be the most efficacious treatment for OSA to date.[22] Prior studies indicate that CPAP manipulation can be used to determine upper airway physiological traits, by alternating between therapeutic and a subtherapeutic level.[23,24] The direct effects of CPAP on soft tissues surrounding the upper airway have been extensively studied using static MRI.[25] However, the underlying mechanisms of airway tissue response to pressure change remains unclear. Due to acquisition speed and spatial coverage constraints, the relationship between soft-tissue collapsibility and physiological traits of OSA are not completely understood.

In this work, we apply and assess a simultaneous multislice (SMS) RT-MRI technique[17] to image and quantify upper airway changes during rapid changes in CPAP pressure level. We use this tool to determine if RT-MRI during CPAP can be used to measure neuromuscular reflex and/or passive collapsibility of the upper airway in individuals with OSA.

Materials and Methods

Experimental Methods

Four adolescent subjects with OSA and obesity (3M/1F), and three healthy volunteers (3M) were studied. The experiment protocol was approved by our Institutional Review Board. Written informed consent was obtained from all adult subjects and volunteers, and obtained from the subject's parents if they were younger than 18 years of age. Subjects were scanned starting at 8 PM, and were instructed to refrain from consuming caffeine for 24 hours prior to the study. Total scan time per subject was 2–4 hours. We performed the experiments on a 3T GE Signa HDxt MRI scanner (GE Healthcare, Waukesha, WI) with gradients capable of 40 mT/m amplitude and 150 T/m/s slew rate. A body coil was used for RF transmission and a 6-channel carotid coil (NeoCoil, Pewaukee, WI) was used for signal reception.

During the MRI scan, we monitored and collected several physiological signals to determine sleep/wakefulness. All instrumentations were either noted as MRI-compatible by the manufacturer or were tested and verified to contain no metallic components by our group. An optical fingertip plethysmograph (Biopac, Goleta, CA) was used to monitor heart rate and oxygen saturation. A respiratory transducer (Biopac) and the scanner's built-in respiratory bellows (GE Healthcare) were used to measure respiratory effort at the lower chest and abdomen.

A facemask (Hans Rudolph, Kansas City, MO) covering both nose and mouth was used to measure airway pressure and for providing positive pressure for CPAP testing. Small-bore tubing from the mask port led to a MP-45 pressure transducer (Validyne Engineering, Northridge, CA) for measurement of mask pressure. The inspiratory port of the mask was connected to a Philips Respironics System One CPAP machine (Respironics, Murrysville, PA) through an extension tube with length of 5 m. Both the CPAP machine and the monitoring devices were located alongside the MRI console to enable the MRI scanner operator to change the mask pressure level during the scan and to monitor sleep/wakefulness in real time during the study.[24]

MRI Protocol

All subjects first underwent overnight polysomnography in a sleep laboratory, which determined the therapeutic CPAP level. During each scan, the CPAP level in the facemask was alternated between the therapeutic value and 4 cm H_2O. Positive pressure of 4 cm H_2O is required to overcome the resistance of the long extension tube connecting CPAP and facemask. A representative scan protocol is shown in Fig. 1. Each scan began with pressure level at 4 cm H_2O. A 10-minute pressure ramp was generated to gradually raise CPAP level from 4 cm H_2O to the predetermined therapeutic level to avoid discomfort. Then the CPAP pressure level was maintained at a therapeutic level to facilitate sleep. The resting airway area (A_{eupnea}) was recorded as an average value across a 20-second time span where pressure was maintained at the therapeutic level. When the CPAP was dropped, there would be an immediate reduction of airway cross sectional area as the airway narrowed. The reduction of airway area (ΔA_d) can be measured by subtracting A_{eupnea} from an average value of airway area during the subtherapeutic period after a 2–3 breaths transition time. This increased upper airway resistance led to an increase in respiratory drive. The effect of this increase on upper airway could be measured when rapidly restoring CPAP back to the therapeutic level, by subtracting the overshoot (ΔA_r) from the resting airway area A_{eupnea}. For a CPAP drop to be used to measure the desired traits, no arousals related to apnea/hypopnea could occur during the subtherapeutic period.[24] This alternating procedure was repeated 2–3 times during each scan, with at least 2-minute intervals, resulting a total scan time of 20–30 minutes.

We used an SMS golden angle radial fast gradient echo sequence to acquire real-time images.[17] This provided 1 mm in-plane spatial resolution and four simultaneous slices (two-retroglossal and two-retropalatal), with 96 msec temporal resolution. Imaging parameters were: 5° flip angle, 200 samples per readout, field of view (FOV) 20 × 20 cm², repetition time / echo time (TR/TE) 3.7/6.5 msec, slice thickness/gap 7/3 mm. Standard static volume
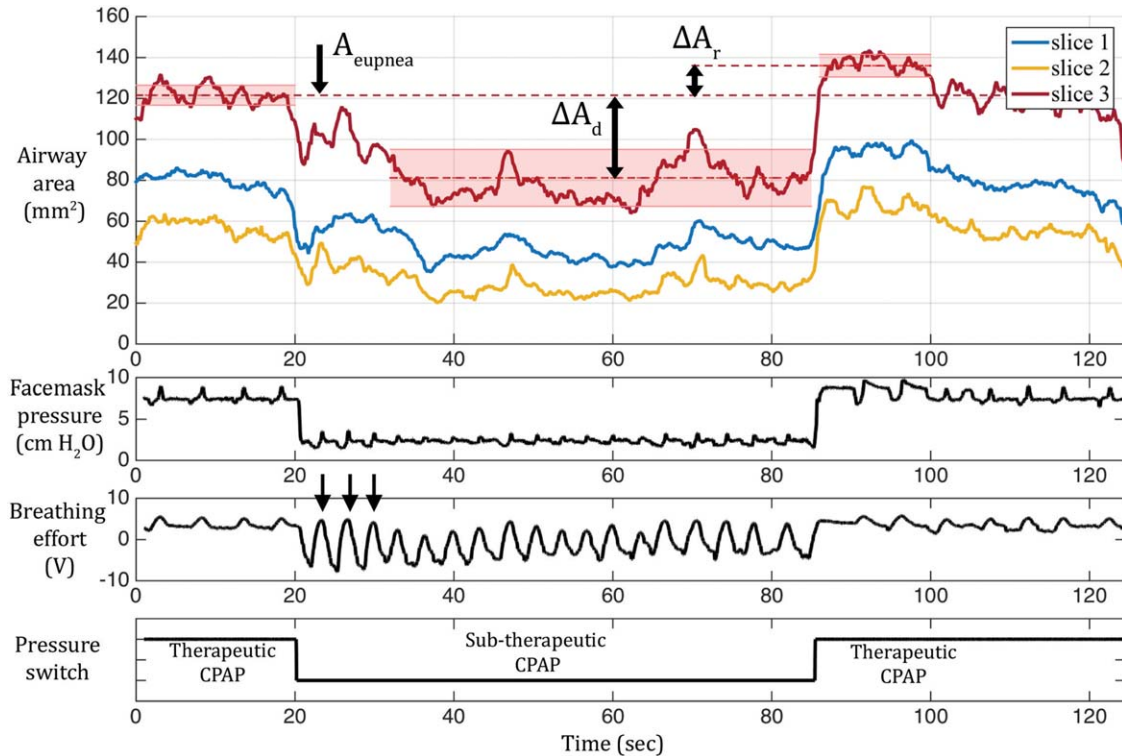
FIGURE 1: CPAP pressure level manipulation. A representative example of CPAP drop/recovery of a healthy volunteer is shown to illustrate physiological changes during the process. Bottom graph shows CPAP being alternated between the predetermined therapeutic level of 8 cm H_2O and the subtherapeutic baseline level of 4 cm H_2O. The effects of this manipulation on airway area, facemask pressure, and breathing effort are shown in the top three graphs. The resting airway area (A_{eupnea}) is determined by averaging the airway area before the CPAP drop. When the CPAP is dropped, there is an immediate narrowing of the airway (ΔA_d), resulting in a ventilation reduction. This reduction in ventilation stimulates the respiratory drive to increase breathing effort. The effect of increased drive on upper airway recovery can be measured by the overshoot of the airway area (ΔA_r) when rapidly recovering CPAP to the therapeutic level after 1 minute. ΔA_r is calculated by subtracting the mean airway area of the first 2–3 breaths after the CPAP recovery from A_{eupnea}.

localizer scans were performed to identify and prescribe the imaging slices.

Data Analysis

We used a semiautomated region-growing algorithm[26] to segment the airway in each 2D slice. We manually placed 2–4 seeds into the airway in each slice for the first time frame. The algorithm then grew a region of interest that included the entire airway for all time frames. Cross-sectional areas were calculated based on the segmented airway.

Figures 1 and 2 show representative examples of a healthy volunteer and an OSA subject, respectively. Upper airway loop gain (UALG) represents the stability of neuromuscular reflex system to recover from sudden ventilation reduction. Note that UALG is distinct from upper airway gain (UAG) defined previously.[24] The latter is a quantification on the airway reflex based on ventilation curves, while UALG is determined by direct measurement of cross-sectional areas. We calculated UALG by taking the ratio of the overshoot ΔA_r to the area drop ΔA_d marked in Fig. 1. This calculation is valid for healthy volunteers and patients whose subtherapeutic section underwent no interruption by apnea/hypopnea events. However, we frequently observed cases where the subtherapeutic period was perturbed by apnea/hypopnea events in OSA patients, as shown in Fig. 2. In such cases, the measurement

accuracy would be reduced by the severe fluctuation of airway if the same method was used. Therefore, we employed a direct measure of airway collapse and reopening.

We identified each apnea/hypopnea event by facemask pressure and bellows signal, highlighted by arrows in Fig. 2. We then averaged across all these time segments to estimate the area drop A_d. Similarly, we located the airway area reopening by examining the facemask pressure curve and detecting the 1–3 breath resurgence after each event. We determined airway reopening ΔA_r by subtracting A_{eupnea} from the average across all of the detected segments. UALG was calculated as the ratio of airway area reopening ΔA_r to the area drop ΔA_d.

The fluctuation of airway area (FAA) represents passive collapsibility of the upper airway. We determined FAA by the standard deviation of airway area normalized by the mean value, in therapeutic and subtherapeutic sections, respectively.

We calculated the mean value and the standard deviation of UALG for each subject to evaluate the stability of neuromuscular reflex system. The mean value and standard deviation of the FAA were also calculated for both OSA patients and control group. We performed Student's t-test between the two groups to evaluate the statistical difference.

To evaluate the intrasubject reproducibility, one OSA patient and one healthy volunteer were removed from the MRI after one
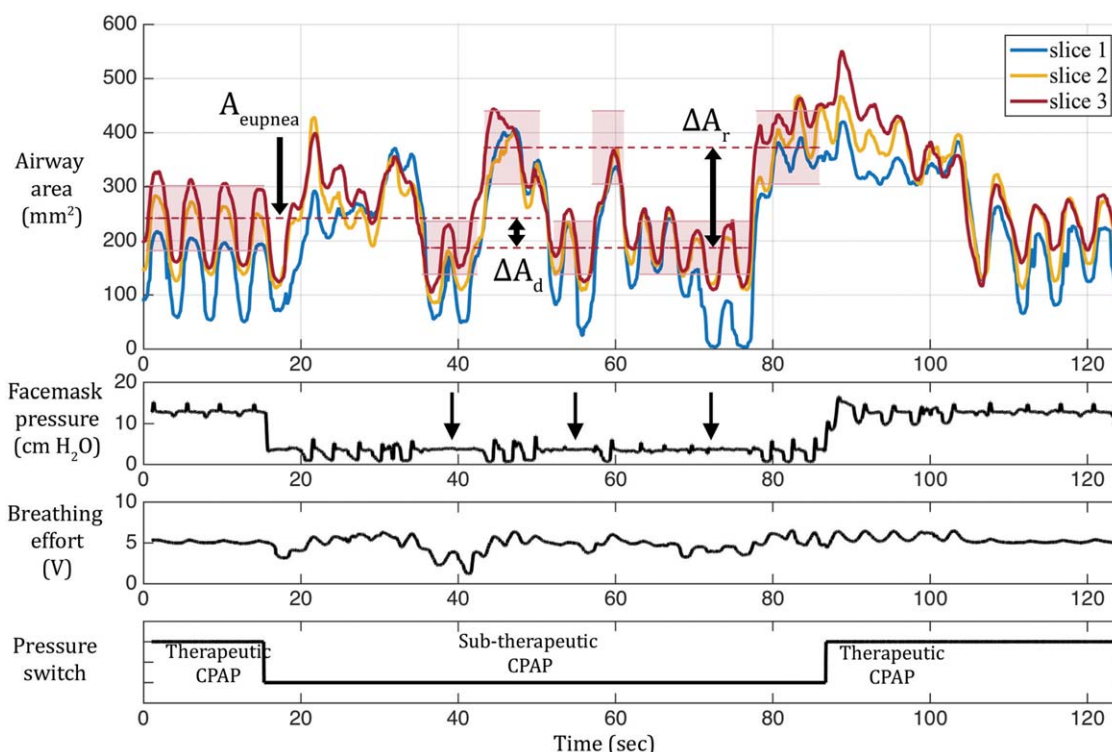
FIGURE 2: Results from a representative OSA patient (male, AHI 50.0, BMI 40.5) illustrate the measurement of airway area change when there are interruptions due to airway collapse. The collapse and recovery of the airway were directly measured when the subtherapeutic interval is interrupted by airway collapse and/or arousal. Apnea/hypopnea events are highlighted by the arrows in facemask pressure curve. The drop ΔA_d was calculated by subtracting the mean value of area across all collapsing sections from the resting airway area A_{eupnea}. The airway recovery in response to the stimulated respiratory drive was determined by measuring the mean value across the 1–3 breaths immediately following the apnea/hypopnea events.

scan, given a short break, and then repositioned into the scanner for a second scan. Results from both scans were then compared. We repeated the measurements by alternating CPAP pressure level three times within each scan. We determined the physiological traits of two adjacent slices, in order to exclude large variation from different airway sites. Intraclass correlation (ICC) between the two scans were calculated.

Results

Figure 1 contains a representative airway area curve from a healthy volunteer. We observed in healthy volunteers that the response of airway area to CPAP pressure change matched the ventilation curves from a previous study.[24]

Figure 2 contains a representative result from an OSA subject. The subtherapeutic section was frequently interrupted by apnea/hypopnea events, compared to the healthy volunteer. Airway recovery was observed at the end of each apnea/hypopnea event, typically across a 1–3 breath time span. The recovery following airway narrowing was noted to be with larger amplitude A_r in almost all cases, compared to the overshoot measured in the control group, indicating a more dramatic change in muscle tone in response to airway collapse. It was also observed that the tidal breath induced fluctuation of cross-sectional area in the OSA patients is at least 2–3$\times$ larger than those in the healthy volunteers.

Figure 3 shows four example frames dynamic MRI during a CPAP drop from the same dataset shown in Fig. 2. Three columns represent three slices, marked with the same color in the localizer image. Four rows marked with (a–d) represent four timepoints, highlighted in the area vs. time curve at bottom left. The images demonstrate that the SMS RT-MRI is able to provide adequate temporal resolution to resolve airway dynamics during dramatic cross-section area fluctuation.

Table 1 lists the UALG and FAA for all subjects. There was no statistically significant difference in UALG between the OSA patients and the control group. However, we observed that OSA subjects with higher apnea/hypopnea index (AHI) value had higher UALG. Table 1 also lists the FAA in the therapeutic and subtherapeutic intervals. The OSA group had more severe fluctuations of airway area, compared to that of the control group.

Table 2 lists representative results from four distinct slices from the OSA subject in Fig. 2, and illustrates the variation among different airway sites. The first slice has the largest UALG and the most dramatic fluctuation during subtherapeutic interval, indicating that it possesses the least stable neuromuscular response and the least stable airway structure, and therefore is likely to be the most collapsible site. This is reinforced by the blue curve in Fig. 2 that
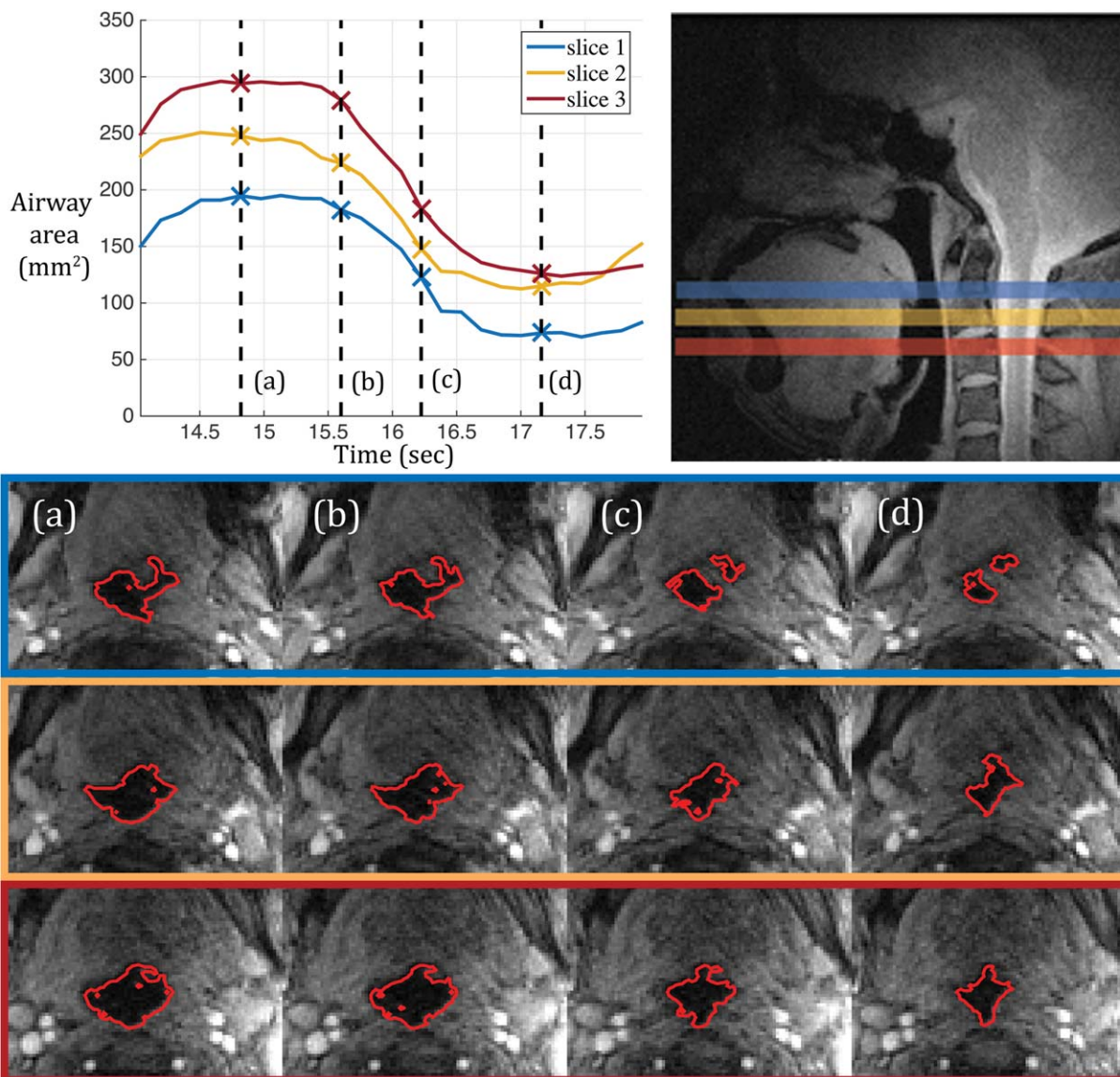
FIGURE 3: RT-MRI during rapid CPAP change. Shown are (bottom row, left to right) four different time points (a–d) marked in the graph (upper left). Red contour shows segmented results in the bottom images. The CPAP was turned to 11 cm H_2O at timepoint (a). The rows correspond to three slices, marked with similar colors in the localizer image (upper right). The airway shape change during tidal breathing at a subtherapeutic pressure, shown in the bottommost two rows, is primarily in the lateral (right–left) direction. This suggests more passive tissue structures exists in the lateral walls, which may be relevant when planning surgical intervention.

shows this slice significantly narrowed and fully collapsed near the 70–80-second interval.

Tables 3 and 4 compare the FAA and mean value of the airway area between the OSA subjects and the control group. Table 3 shows that the airway from the two groups underwent statistically different fluctuation characteristics with P-values less than 0.05 for both subtherapeutic and therapeutic sections. Table 4 shows that the two groups possess the same range of airway size during the subtherapeutic section with no statistically significant difference ($P = 0.672$). However, the right column shows that CPAP remarkably dilate the airway for OSA patients during the therapeutic section, due to their less stable airways.

Table 5 shows representative results for intrasubject reproducibility. Although UALG had large standard deviations across different airway sites for each subject, the intrasubject test–retest result indicates good repeatability within adjacent slices for both the OSA patient (ICC = 0.714) and the healthy volunteer (ICC = 0.757). ICC for FAA were all higher than 0.76, indicating good reliability of the measurements.

Discussion

We present a novel MRI-based experiment that measures UALG and FAA, which are valuable for the study of sleep-related breathing disorders. We utilized SMS RT-MRI, and

TABLE 1. Upper Airway Loop Gain (UALG) and Fluctuation of Airway Area (FAA) Comparison Between OSA Patients and the Control Group

	Gender	AHI (events/Hr.)	UALG	FAA Subtherapeutic	FAA Therapeutic
OSA #1	M	17.3	0.16 ± 0.12	44.8%	15.7%
OSA #2	M	50.0	3.01 ± 1.61	37.2%	25.5%
OSA #3	F	81.8	4.71 ± 4.96	48.6%	22.1%
OSA #4	M	10.3	0.60 ± 0.42	28.8%	9.7%
Control #1	M	—	0.42 ± 0.41	10.5%	4.0%
Control #2	M	—	1.60 ± 1.49	13.6%	9.2%
Control #3	M	—	1.60 ± 2.16	13.0%	5.0%

There was no clear difference in UALG between the two groups. However, OSA subjects with higher apnea/hypopnea index (AHI) tended to have larger UALG, which implies a less stable neuromuscular control system in the upper airway. There was a significant difference (see Table 3) in FAA between the two groups, indicating that OSA patients in the cohort had more collapsible and less stable airways.

CPAP with carefully designed pressure changes. This new test is valuable because conventional PSG with AHI measurement only provides estimation of the overall severity of OSA and cannot localize specific airway sites that are prone to collapse. In contrast, the proposed experimental design can directly measure location-specific active (UALG) and passive (FAA) physiological traits, and visually resolve airway dynamics.

We observed that OSA subjects with higher AHI had higher UALG, suggesting that the OSA cohort have less stable neuromuscular control systems of their upper airways. The OSA group also exhibited larger fluctuations of airway area, compared to that of the control group. This suggests that OSA subjects in the cohort possess less stable airways with greater collapsibility.

TABLE 2. UALG and FAA Results for Different Slices of One Representative OSA Patient

Slice	UALG	FAA Subtherapeutic	FAA Therapeutic
1	4.21 ± 1.16	40.6%	27.2%
2	2.59 ± 0.93	33.1%	24.3%
3	2.57 ± 0.91	29.4%	28.8%
4	1.80 ± 0.21	32.4%	27.6%

We list results from four axial slices from one representative OSA patient to illustrate the variation among airway sites. Slice #1 has the largest UALG and FAA during the subtherapeutic section, indicating it possessed the least stable neuromuscular reflection and the most passive airway tissue, and therefore was the most collapsible site.

Occlusion studies can potentially measure biomarkers for passive and anatomical risk factor for OSA, such as closing pressure and compliance.[17,27] In addition to these measurements, we demonstrate that the proposed experiment has the potential to estimate the active factors of upper airway in response to collapse. Furthermore, CPAP provides accurate pressure control, while occlusion studies produce negative pressure only and suffer from more variability due to inconsistent volunteer respiratory effort.

It is possible to scan patients during wakefulness with occasional occlusions[17]; however, we have found CPAP to be more patient-friendly. Previously, subjects reported discomfort introduced by short-time occlusions during wakefulness. Patients with OSA typically have previous CPAP experience, which facilitates comfort and the likelihood of sleep in the MRI scanner. We gradually increased the pressure level before the scan procedure, in order to minimize the chance of interrupting sleep. In our experience, all subjects did fall asleep during MRI scanning while wearing the CPAP apparatus (four of four patients and three of three volunteers in this study).

It is important to measure active muscle reaction to airway collapse during natural sleep. During wakefulness, there is additional variability in UALG measurement. We speculate this is due to different neuromuscular mechanisms during wakefulness, stiffer muscle tone, and airway motion due to swallowing. We observed differences between measured UALG and FAA between sleep and wakefulness for all subjects. Specifically, we observed that during wakefulness, reopening is restrained, and the overshoot after CPAP recovery is reduced.

Previous studies[4,24,28] that used PSG and CPAP to determine physiological traits had to exclude significant

TABLE 3. Fluctuation of Airway Area (FAA) Between OSA Subjects and the Control Group

	Quantity	FAA Subtherapeutic	FAA Therapeutic
OSA	4	42.6%±9.4%	18.3%±7.0%
Control	3	13.6%±0.6% ($P = 0.003$)	6.2%±2.6% ($P = 0.04$)

Shown are the FAA during the subtherapeutic and therapeutic sections. There was a statistically significant difference between the OSA and control group (Student's t-test, $P < 0.05$) for both sections. Increasing CPAP pressure, as done in the therapeutic section, reduced the magnitude of the difference.

TABLE 4. Airway Area Mean Value

	Quantity	Airway area mean value Subtherapeutic	Airway area mean value Therapeutic
OSA	4	83.3 ± 53.7	147.1 ± 72.6
Control	3	79.1 ± 51.1 (p = 0.672)	110.8 ± 65.1 (p = 0.007)

A Student's t-test was used to compare the mean airway area during the subtherapeutic and the therapeutic sections. There was no significant difference between the 2 groups during the subtherapeutic section. CPAP was able to remarkably dilate the airway for OSA patients, who possess more passive airways. This implies that airway stiffness, instead of the anatomic profile, has an important role in maintaining airway patency in the sampled OSA cohort.

amounts of data where there were arousal interruptions. In those studies, the measurements of airway reaction were based on physiological modeling and the assumption that the ventilation drive compensation to CPAP drop is due to a reopened airway. Our observation (for all OSA patients and healthy volunteers) was that the airway did not necessarily reopen in response to the CPAP drop, unless the airway itself underwent significant narrowing or total collapse. This could mean that: 1) either the assumption in the previous studies is not correct; or 2) that the subjects were not in a stable and sufficiently deep stage of sleep. In both cases, the upper airway never become totally passive. This

observation was made possible because the proposed MRI experiment includes direct measurement of cross-sectional area. Previous studies using static MRI have shown enlarged airway area with progressively increased pressure.[25,29] However, with improved spatial coverage and enhanced temporal resolution, the fully resolved dynamics reveal that airway area depends on many factors in addition to the pressure level, including specific airway section and muscle tone status.

The upper airway includes the pharynx, which is a structural and physiologically complicated system serving multiple functions. Also, OSA is a heterogeneous syndrome,

TABLE 5. Intrasubject Reproducibility

		UALG	FAA Subtherapeutic	FAA Therapeutic
OSA	Scan 1	2.94 ± 0.72	27.3%±3.1%	24.9%±1.6%
	Scan 2	2.65 ± 1.51	31.2%±4.1%	20.7%±4.5%
	ICC	0.714	0.823	0.761
Control	Scan 1	0.19 ± 0.06	7.6%±1.5%	3.1%±1.0%
	Scan 2	0.21 ± 0.14	7.9%±1.7%	3.3%±1.2%
	ICC	0.757	0.865	0.878

One OSA patient and one control volunteer were scanned twice in the same session, with subject removal and replacement, to determine intrasubject test-retest reproducibility. Two adjacent slices were used. For each scan, the measurements were repeated by alternating CPAP pressure level 3 times. Intraclass correlation (ICC) for UALG and FAA measurements were calculated for both subjects.

with several structural and physiological pathways.[30,31] Therefore, we expect variation in both UALG and FAA across different airway sites. This study documented large variability in these quantities across patients and slice locations. This establishes the value and importance of using simultaneous multislice imaging for this application. We observed OSA 2,3 had 3–8× larger UALG than OSA 1,4, and OSA 1,2,3 had 1.5–3× larger FAA than OSA 4. We speculate that these large variations are due to weighting of active/physiological and passive/anatomical factors for these subjects, because they represent different phenotypes and severities of OSA. We also observed large intrasubject variation; for example, for OSA 2 slice 1 has the largest value for both UALG and FAA. This potentially indicates slice 1 should be given higher priority for treatment. These observations suggest the possibility of personalized treatment for OSA patients.[31]

This preliminary study has several limitations. First of all, we had a small cohort (four patients and three controls), and the findings need to be confirmed in a larger sample. Second, we used a relatively large slice thickness of 7 mm, which is insufficient to fully resolve the motion of certain interesting structures, such as uvula, during airway collapse. This in combination with the 3 mm slice gap makes it difficult to tackle transplane motion, which could introduce additional bias/variation. Third, our 2D area segmentation is based on a region-growing algorithm, and was not optimized to overcome rapid movement of the subject. In rare cases we needed to manually segment the airway when adjacent frames did not possess adequate airway overlap. 3D segmentation[32] with improved spatial coverage and adequate resolutions is in demand and remains for future work. Fourth, this experiment would benefit from natural sleep in the scanner; however, this is not always practical.

In conclusion, we demonstrate a novel experiment that can simultaneously measure upper airway active and passive traits regarding OSA, including physiological and anatomical factors, potentially enabling detailed phenotyping of OSA patients. By performing SMS RT-MRI during CPAP, we reveal that airway behavior in OSA patients possesses large variation. Patients may deserve personalized examination before proceeding to specific treatment. We also demonstrate the proposed experiment can help locate the most collapsible airway sites with higher treatment priority, with specific possible reasons (anatomical or physiological). With these demonstrated result, we also expect that this experiment can be further used in other procedures, such as detailed CPAP titration or aiding in surgery planning.

Acknowledgment

References

1. White DP. Central Sleep Apnea. In: Principles and Practice of Sleep Medicine. Philadelphia: Elsevier. 2005:969–982.

2. Arens R, Marcus CL. Pathophysiology of upper airway obstruction: a developmental perspective. Sleep 2004;27:997–1019.

3. Harvard Medical School, McKinsey. The Price of Fatigue: The Surprising Economic Costs of Unmanaged Sleep Apnea. Cambridge, MA: Harvard Press; 2010.

4. Young T, Peppard PE, Gottlieb DJ. Epidemiology of obstructive sleep apnea: A population health perspective. Am J Respir Crit Care Med 2002:1217–1239.

5. Andreas S, Schulz R, Werner GS, Kreuzer H. Prevalence of obstructive sleep apnoea in patients with coronary artery disease. Coron Artery Dis 1996;7:541–545.

6. Javaheri S, Parker TJ, Liming JD, et al. Sleep apnea in 81 ambulatory male patients with stable heart failure. Types and their prevalences, consequences, and presentations. Circulation 1998;97:2154–2159.

7. Guilleminault C, Connolly SJ, Winkle RA. Cardiac arrhythmia and conduction disturbances during sleep in 400 patients with sleep apnea syndrome. Am J Cardiol 1983:490–494.

8. Bradley TD, Logan AG, Kimoff RJ, et al. Continuous positive airway pressure for central sleep apnea and heart failure. N Engl J Med 2005;353:2025–2033.

9. Ip MSM, Lam B, Ng MMT, Lam WK, Tsang KWT, Lam KSL. Obstructive sleep apnea is independently associated with insulin resistance. Am J Respir Crit Care Med 2002;165:670–676.

10. Punjabi NM, Sorkin JD, Katzel LI, Goldberg AP, Schwartz AR, Smith PL. Sleep-disordered breathing and insulin resistance in middle-aged and overweight men. Am J Respir Crit Care Med 2002;165:677–682.

11. Strollo PJ, Rogers R. Obstructive sleep apnea. Curr Treat Options Neurol 1996;334:99–104.

12. Sforza E, Bacon W, Weiss T, Thibault A, Petiau C, Krieger J. Upper airway collapsibility and cephalometric variables in patients with obstructive sleep Apnea. Am J Respir Crit Care Med 2000;161(2 I):347–352.

13. Arens R, McDonough JM, Costarino AT, et al. Magnetic resonance imaging of the upper airway structure of children with obstructive sleep apnea syndrome. Am J Respir Crit Care Med 2001;164:698–703.

14. Schwab RJ, Pasirstein M, Pierson R, et al. Identification of upper airway anatomic risk factors for obstructive sleep apnea with volumetric magnetic resonance imaging. Am J Respir Crit Care Med 2003;168:522–530.

15. Wagshul ME, Sin S, Lipton ML, Shifteh K, Arens R. Novel retrospective, respiratory-gating method enables 3D, high resolution, dynamic imaging of the upper airway during tidal breathing. Magn Reson Med 2013;70:1580–1590.

16. Kim Y-C, Lebel RM, Wu Z, Ward SLD, Khoo MCK, Nayak KS. Real-time 3D magnetic resonance imaging of the pharyngeal airway in sleep apnea. Magn Reson Med 2014;71:1501–1510.

17. Wu Z, Chen W, Khoo MCK, Davidson Ward SL, Nayak KS. Evaluation of upper airway collapsibility using real-time MRI. J Magn Reson Imaging 2016;44:158–167.

18. Kushida CA, Littner MR, Morgenthaler T, et al. Practice parameters for the indications for polysomnography and related procedures: an update for 2005. Sleep 2005;28:499–521.

19. Terris DJ, Hanasono MM, Liu YC. Reliability of the Muller maneuver and its association with sleep-disordered breathing. Laryngoscope 2000;110:1819–1823.

20. Pang KP, Terris DJ. Multilevel pharyngeal surgery for obstructive sleep apnea. In: Friedman M, ed. Sleep Apnea Snoring Surgical and Non-surgical Therapy. Amsterdam: Elsevier; 2009:268–278.

21. Fujita S. Surgical treatment of OSA: UPPP and lingualplasty (laser mid-line glossectomy). In: Guilleminault C, Partinen M, eds. Obstructive Sleep Apnea Syndrome Clinicial Research and Treatment. New York: Raven Press; 1990:129–151.

22. Semelka M, Wilson J, Floyd R. Diagnosis and treatment of obstructive sleep apnea in adults. Am Fam Physician 2016;94:355–360.

23. Wellman A, Eckert DJ, Jordan AS, et al. A method for measuring and modeling the physiological traits causing obstructive sleep apnea. J Appl Physiol 2011;110:1627–1637.

24. Edwards B a, Wellman A, Sands SA, et al. Obstructive sleep apnea in older adults is a distinctly different physiological phenotype. Sleep 2014;37:1227–1236.

25. Schwab RJ. Upper airway imaging. Clin Chest Med 1998;19:33–54.

26. Kim Y-C, Wang X, Tran W, Khoo MCK, Nayak KS. Measurement of upper airway compliance using dynamic MRI. In: Proc 20th Annual Meeting ISMRM, Melbourne; 2012. p 3688.

27. Issa FG, Sullivan CE. Upper airway closing pressures in obstructive sleep apnea. J Appl Physiol 1984;57:520–527.

28. Salloum A, Rowley JA, Mateika JH, Chowdhuri S, Omran Q, Badr MS. Increased propensity for central apneas in patients with obstructive sleep apnea. Effect of nasal continuous positive airway pressure. Am J Respir Crit Care Med 2010;181:189–193.

29. Ahmed MM, Schwab RJ. Upper airway imaging in obstructive sleep apnea. Curr Opin Pulm Med 2006;12:397–401.

30. Caples SM, Gami AS, Somers VK. Obstructive sleep apnea. Ann Intern Med 2005;142:187–197.

31. Pack AI. Application of personalized, predictive, preventative, and participatory (P4) medicine to obstructive sleep apnea. A roadmap for improving care? Ann Am Thorac Soc 2016;13:1456–1467.

32. Javed A, Kim YC, Khoo MCK, Ward SLD, Nayak KS. Dynamic 3-D MR visualization and detection of upper airway obstruction during sleep using region-growing segmentation. IEEE Trans Biomed Eng 2016:431–437.